



ISSN: 0976-3376

Available Online at <http://www.journalajst.com>

ASIAN JOURNAL OF
SCIENCE AND TECHNOLOGY

Asian Journal of Science and Technology
Vol. 16, Issue, 01, pp. 13381-13387, January, 2025

RESEARCH ARTICLE

GEOLOGICAL AND STRUCTURAL MAPPING OF THE OUADDAÏ MASSIF USING LANDSAT AND RADAR DATA

NGAMBI Victor HINGUE^{1*}, MBAGUEDJE Diondoh² DOUMNANG MBAIGANE Jean Claude¹, ALLARASSEM Lutian¹BALLADURE MBAIADE¹, and Diontar MBAIHOUDOU³

¹Laboratory of Geology, Geomorphology and Remote Sensing, University of N'djamena/Chad

²Department of Geology, Adam Barka University, Abéché/Chad

³Department of Geology, Mongo Polytechnic University/Chad

ARTICLE INFO

Article History:

Received 11th November, 2024

Received in revised form

09th December, 2024

Accepted 20th December, 2024

Published online 22nd January, 2025

Keywords:

Mapping, Remote sensing,
Ouaddaï massif,
Eastern Chad and lineament.

ABSTRACT

The aim of the work was to produce a geological and structural map of the Ouaddaï massif using landsat and radar data. We used landsat-8 images to extract the lithological map (colour composition and ratio bands) and PALSAR DEM radar to extract the lineament map (using different filters). For the radar sensor, a total of 2188 lineaments were detected and extracted, with two main rock fracturing directions (ESE-WNW (90° to 115°) and NE-SW (45° to 65°)). For the landsat-8 sensor, a total of 987 lineaments were extracted, with two main lineament directions (NE-SW or N45° to 65° and ENE-WSW or 115° to 135°). Field observation revealed that the geological bedrock in the eastern part of the Ouaddaï massif is mainly granitic. The NE-SW and SE-NW directions are the main fracturing directions in these geological formations.

Citation: MBAGUEDJE Diondoh, NGAMBI Victor HINGUE, DOUMNANG MBAIGANE Jean Claude, ALLARASSEM Lutian and Diontar MBAIHOUDOU. 2025. "Geological and Structural Mapping of the Ouaddaï Massif using Landsat and Radar Data", *Asian Journal of Science and Technology*, 16, (01), 13381-13387.

Copyright©2025, MBAGUEDJE Diondoh et al. This is an open access article distributed under the Creative Commons Attribution License, which permits unrestricted use, distribution, and reproduction in any medium, provided the original work is properly cited.

INTRODUCTION

One of the most successful aspects of prospecting for natural resources is mapping the lithological units that make up the subsoil. The study of mapping requires the characterisation and recognition of the maximum number of outcrops likely to provide information and results on the nature of the geological substratum (Baghdadi *et al.*, 2005). Image processing using remote sensing techniques is an important approach in geological studies (El-Sawy *et al.*, 2016; Hammad, 2016). To date, several studies have demonstrated the usefulness of remote sensing methods in mapping lineaments, which are considered to be important tectonic and structural indicators for determining regional and tectonic trends in fracture zones in rocks (El-Sawy *et al.*, 2016); (Miyouna *et al.*, 2020). Several studies have demonstrated the usefulness of radar and optical sensors for geological, hydrogeological and mining studies (Baghdadi *et al.*, 2005; Kruse *et al.*, 2003). The information provided by the sensors facilitates the description and interpretation of geological structures. The contribution of radar imagery has also become very important in the study of arid and semi-arid zones. In these areas, radar waves penetrate spectral surfaces (stratum, soil, rock, fossil) and thus highlight geological structures in the middle or buried in hydrographic networks (Berraki *et al.*, 2012); (Djerosse *et al.*, 2024). Another technique for exploring natural resources is the classical geological study (petrography, structural). Based on the colour composition, band ratios and lineaments generated from the

optical (Landsat-8) and radiometric (Radar) sensors, the lineament map was drawn up. Observation revealed that the geological bedrock in the eastern part of the Ouaddaï massif is predominantly granitic. The NE-SW and SE-NW directions are the main fracturing directions of these geological formations. Fieldwork has shown that the geological formations in the study area are almost entirely composed of granitoids (granite, granodiorite, diorite). They outcrop in slabs, balls and domes ranging in size from metric to kilometric. The structural analysis carried out showed that the geological formations do not have enough kinematic and dynamic markers visible at the outcrop and rock scale.

Geological context: The study area is located in eastern Chad in the province of Ouaddaï, department of Asounhga. It lies between latitudes 13°15' and 13°45' North and between longitudes 21°24' and 22°2' East. Mining and geological prospecting work has been carried out by Gsell and Sonet, 1960; Chaussier, 1970; Kusnir, 1995; Djerosse, 2018; De Wit *et al.*, 2021. The Ouaddaï massif is underlain by a Precambrian basement, consisting of metasedimentary and metavolcanic rocks, and plutonic rocks of intermediate to felsic composition, forming plutons and veins intersecting the metamorphic rocks (Gsell J and Sonnet J., 1960); (Kusnir, 1995), (Fig. 1). This massif is mainly granitic and migmatitic (Chaussier, 1970; Hingue *et al.*, 2024; Pias, 1964; Schneider, 2001). Towards the south of the massif, rocks outcrop in abundance. They consist of gneisses (type-S leucogranites, type-I calc-alkaline potassic granitoids) and metasedimentary rocks (amphibolites, greenschists), (Djerosse, 2018); (Djerosse *et al.*, 2020). The northern part of the Ouaddaï massif is described as consisting mainly of granitoids and migmatites

*Corresponding author: NGAMBI Victor HINGUE

Laboratory of Geology, Geomorphology and Remote Sensing, University of N'djamena/Chad

interspersed with volcano-sedimentary rocks. The north-eastern part of the massif is generally composed of quartzite, pelites, schist, amphibolites, paragneiss and occasionally marble (De Wit *et al.*, 2021). The western part of the Ouaddaï massif is largely dominated by post-tectonic intrusive granitoids, alkaline granites, monzonites and syenites. Metavolcanosedimentary rocks are rare in this area compared with the eastern part of the massif (De Wit *et al.*, 2021). The eastern part of the massif is described by (Hingue *et al.*, 2024) as consisting mainly of granite and diorite. These granitoids are metaluminous, calc-alkaline and belong to the type-I granitoids with an iron-bearing character. The structural and morpho-structural analysis revealed three (03) deformation phases. The first, characterised by horizontal foliation S1. The second phase is marked by schistosity/foliation S2 corresponding to axial plane schistosity, associated with mineral lineations and NNE-SSW direction stretches, P2 isopaque folds and asymmetric folds and boudins with dexter displacement. The third phase is marked by the development of shears and joints, and its tectonics is brittle (Oussama, 2023). The work of (Al-Djazouli *et al.*, 2019) has shown that fracture zones in basement regions are essential for understanding groundwater corridors and traps.

MATERIALS AND METHODS

MATERIALS

We used several cartographic databases for this work

- a 1:500,000 scale geological reconnaissance map of Adré, published by the Institut Equatorial des Recherches et d'Etudes Géologiques et Minières by Gsell and Sonet, 1960, based on a 1:200,000 scale photograph from the Institut Géographique National;
- Landsat-8 images, captured on 04 March 2023 under favourable weather conditions. This scene covers an area of 184 km². It belongs to zone 34 North of the Universal Transverse Mercator (UTM, zone 34 N) map projection and uses the WGS 84 geodetic reference system;
- PALSAR DEM images (12m resolution). This digital terrain model is included in the ALOS PALSAR image file captured on

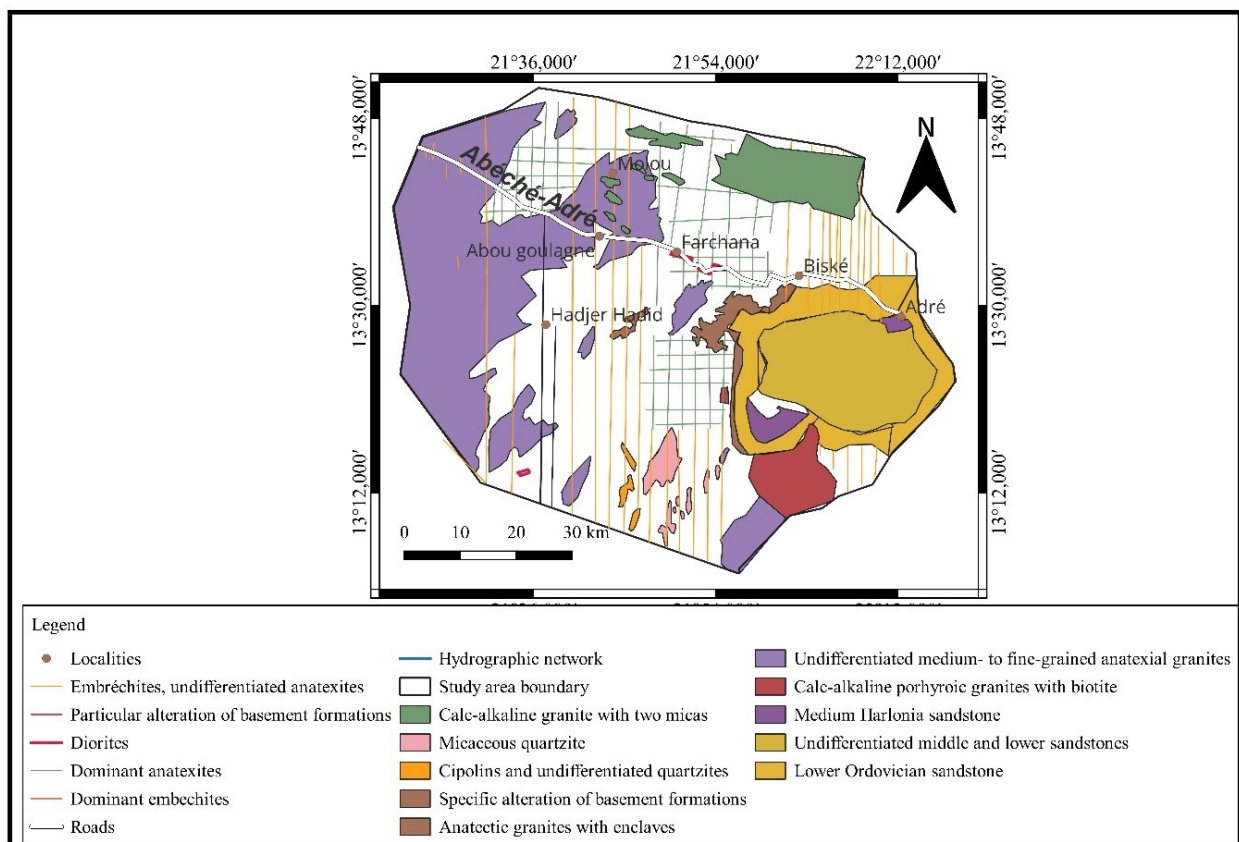


Figure 1. Geological map of the Adré sheet, drawn up by Gsell and Sonet, 1960, adapted

Table 1. Landsats-8/LDCM band characteristics

Instrument OLI		
Bandes spectrales	Longueur d'onde (µm)	Resolution (m)
Bande 1- Aerosols	0,433 - 0,453	30
Bande 2-Bleue	0,450 - 0,515	30
Bande 3- Vert	0,525 - 0,600	30
Bande 4-Rouge	0,630 - 0,680	30
Bande 5- Rouge-Infrarouge	0,845 - 0,885	30
Bande 6 - Infrarouge moyen 1	1,560 - 1,660	30
Bande 7- Infrarouge moyen 2	2,100 - 2,300	30
Bande 8 - Panchromatique	0,500 - 0,680	30
Bande 9 - Cirrus	1,360 - 1,390	30
Instrument TIRS		
Bande 10-Infrarouge moyen	10,30 - 11,30	100
Bande 11-Infrarouge moyen	11,50 - 12,50	100

27 March 2007, downloaded from the NASA/Earth Data portal. Because of its very high spatial resolution, we used PALSAR DEM to make geometric corrections to the HV-polarised radar images.

- This map is supplemented by Aster images GLSDEM_n013e021.tif captured on 28 November 2020, with a resolution of 30 m;
- Vector data (shapefiles). The vector data includes the administrative boundaries of the study area, localities, watercourses and roads; and a fairly diverse bibliography, constituting the basic material for this work.

METHODOLOGY

This phase comprises two stages: the pre-processing or preliminary phase and the processing phase.

Pre-processing of Landsat-8 and radar images

Characteristics of Landsat-8 bands: These satellite images were chosen for their spectral and spatial characteristics, which allow good structural mapping on a small scale. These are bands with good resolutions, the characteristics of which are defined in the table opposite

Geometric correction: The aim of geometric correction is to bring images back to planimetric reality. For landsat-8, geometric correction consisted of correcting and minimising sensor noise and distortion. This also makes it possible to clean up the image and align it with the topographic background of the study area. The sensor is adjusted to the same map projection as the study area, UTM zone 34N. Radar images (H V) were subjected to radiometric calibration and Lee 7x7 filtering using SNAP software.

Landsat-8 OLI image processing: We performed a true-colour composite using combinations of bands 654, 751 and 423. For band ratios, they are techniques that divide a radiometric value of a pixel in one band by the radiometric value of a pixel in another band ((Yang'tshi et al., 2018). Band ratios are a very effective method of distinguishing between two types of rock, because the differences in the near infrared and visible wavelengths lie in the slopes of the reflectivity curves. Band ratios of 6/5, 4/5, 1/6 and 6/7, 6/2 and 6/5 were carried out.

Automatic lineament mapping

Principal component analysis: Principal component analysis is a method of synthesising information (Guerrien, 2003), which is very useful in remote sensing when there is a large quantity of multispectral data to process and interpret. It reduces the information contained in several highly correlated bands to a small number of components (Coulbaly, 1996). Principal component analysis has made it possible to extract the same information from the colour composition and band ratios. The precision of the images obtained by PCA in RGB mode lies at the level of contact and the contours between the different geological formations.

Directional filters: This is used to identify lineaments corresponding to structural or lithological discontinuities in a region (Berraki et al., 2012). In this work we used enhancement in four directions (the 0°, 45°, 90° and 180° filters) because of the high contrast obtained in the images.

Directional rosette: After extracting the lineaments in Geomatica V9.1, we exported the files to Arcgis where the arrival and departure coordinates of all the lineaments were taken. From Arcgis, all the start files were converted into DXF format. These were then imported into Rockworks 17, where the various fracture directions were automatically extracted in the form of a distribution rosette.

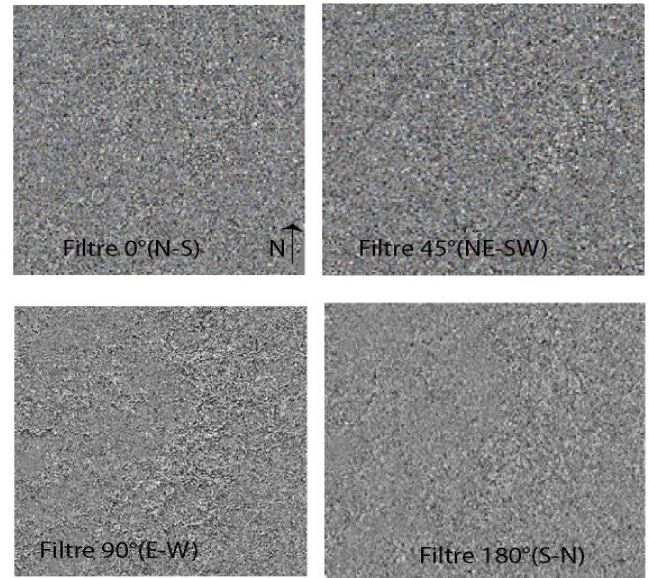


Figure 2. Directional filters

The different methods used in this work are summarised in the figure below (Fig. 3)

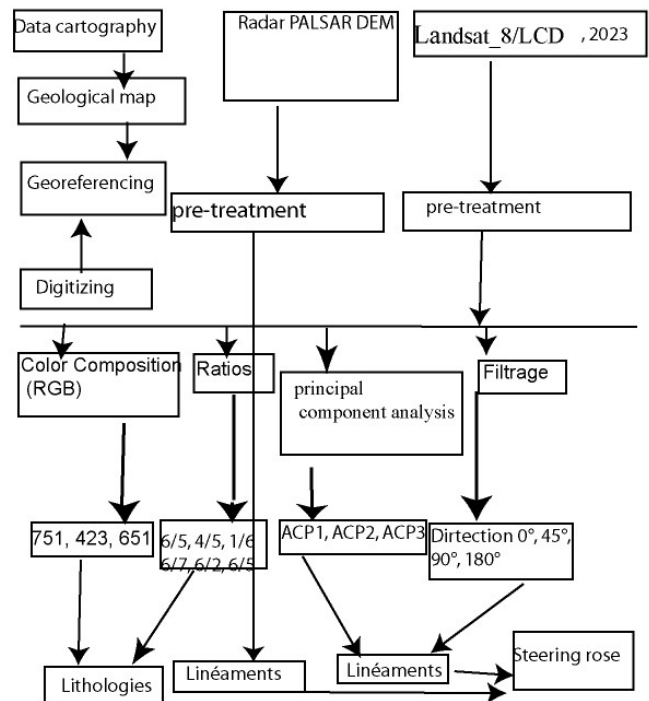


Figure 3. Flowchart of image processing techniques this study

RESULTS

Remote sensing data

Lithology: In terms of colour composition, the vegetation appears red, the alluvium white and the granitoids multi-coloured yellow red brown (Fig 4.). Different colours were observed for the ratio bands. The granitoids in our sector appear as multi-coloured yellow, red and green (Fig.5).

Lineaments: By superimposing filters in different directions, we were able to produce the lineament map using Géomatica and Arcgis software. Extraction was carried out automatically.

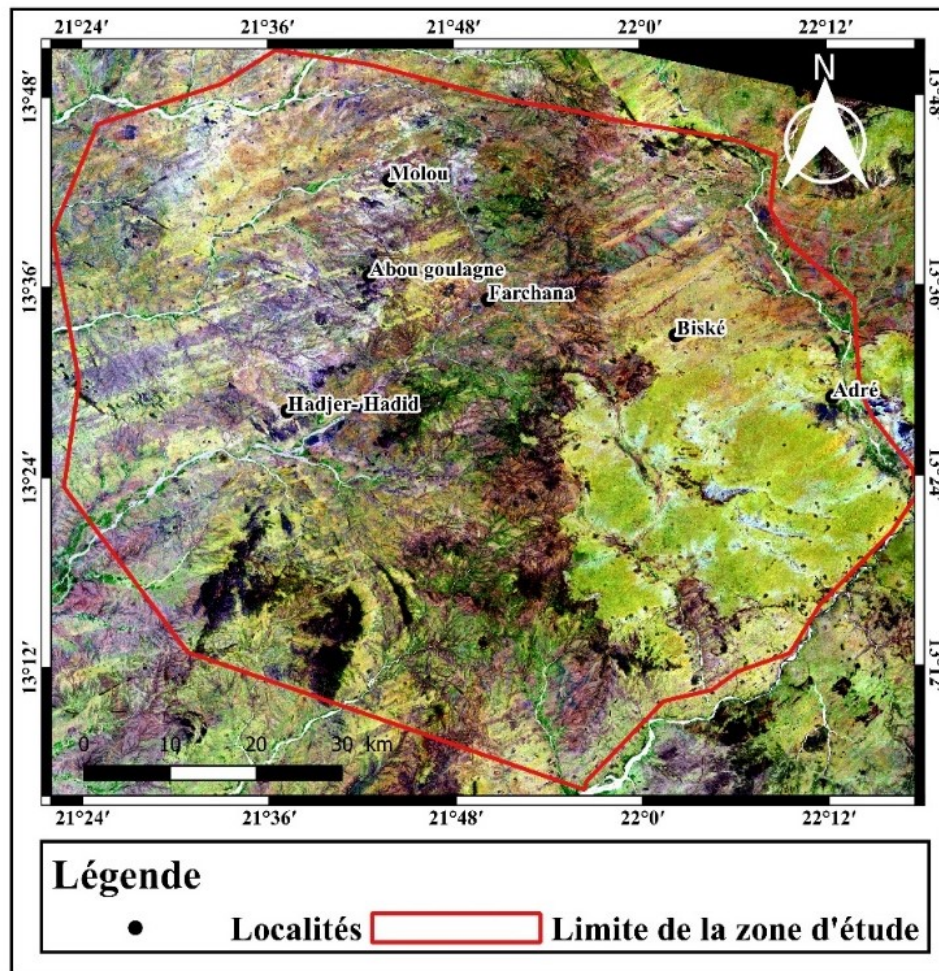


Figure 4. Color composition 651 of the study area

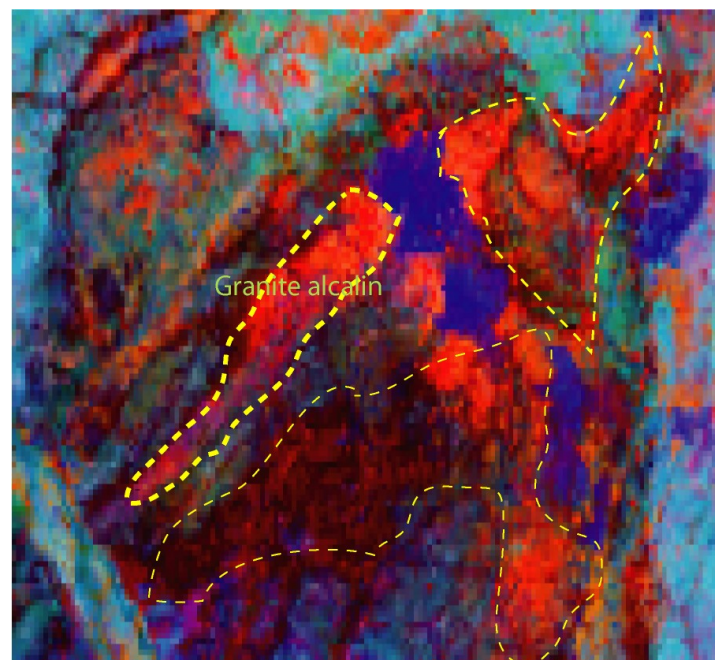


Figure 5. Zoom on the 6/7, 6/2 and 6/5 ratio bands of alkaline granite

This lineament map is therefore the set of unique segments resulting from the stacking and synthesis of information contained in the four filtered images. A total of 987 lineaments were extracted from landsat-8 (Fig. 6). Analysis of the distribution rosette shows that the lineaments are scattered in all directions. However, a few main lineament directions stand out.

These are: NNE-SSW (0° to 23°), NE-SW (45° to 65°), ESE-WNW (90° to 115°), SE-NW (115° to 135°) and SSE-NNW (165° to 180°). These directions include two main fracturing directions: $N45^{\circ}$ to 65° and 115° to 135° , and three secondary directions: $N0^{\circ}$ to 23° , $N90^{\circ}$ to 115° and 165° to 180° =(Fig.7).

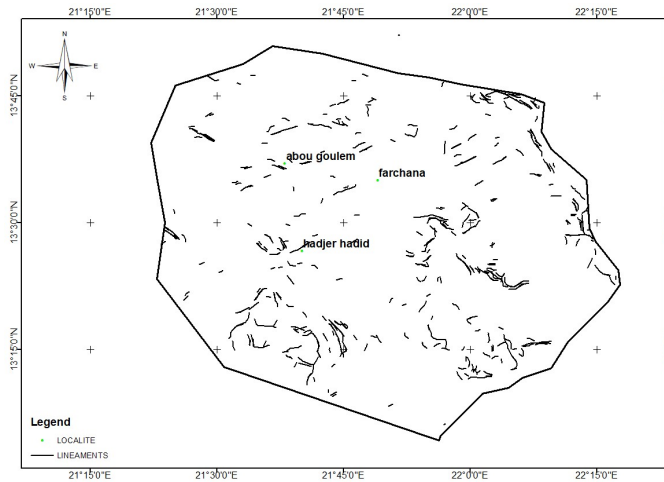


Figure 6. Lineament map extracted from landsat-8

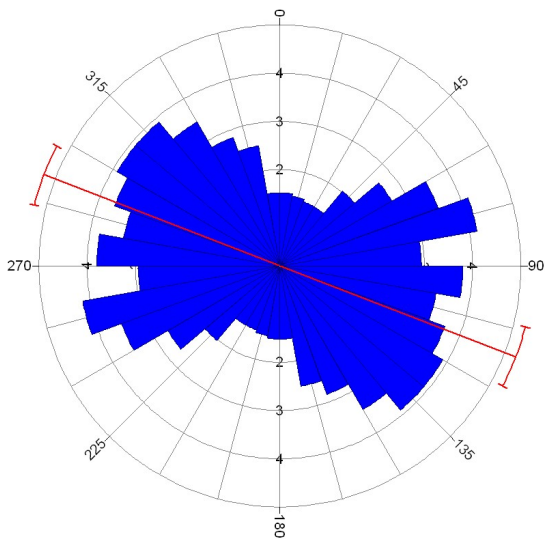


Figure 7. Directional rosette extracted from landsat-8

To reassure ourselves of the reliability of the sensors in providing maximum information on the geological bedrock of the eastern Ouaddaï massif, we used images from the PALSAR DEM radar sensor satellites (cross-polarised, HV). For the radar sensor, a total of 2188 lineaments were detected and extracted (Fig.8).

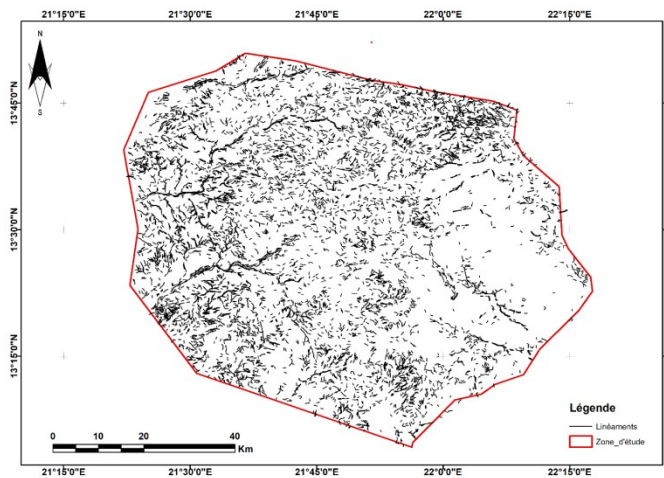


Figure 8. Lineament map extracted from radar PALSAR DEM

Analysis of the distribution rosette shows that the lineaments are scattered in all directions, with precision and clarity.

However, a few main lineament directions stand out. These are: ESE-WNW (90° to 115°), NE-SW (45° to 65°), ESE-WNW and SSE-NNW (165° to 180°). Among these directions, two main ones stand out:

ESE-WNW (90° to 115°) and NE-SW (45° to 65°) and secondary directions ESE-WNW and SSE-NNW (165° to 180°), (Fig.09).

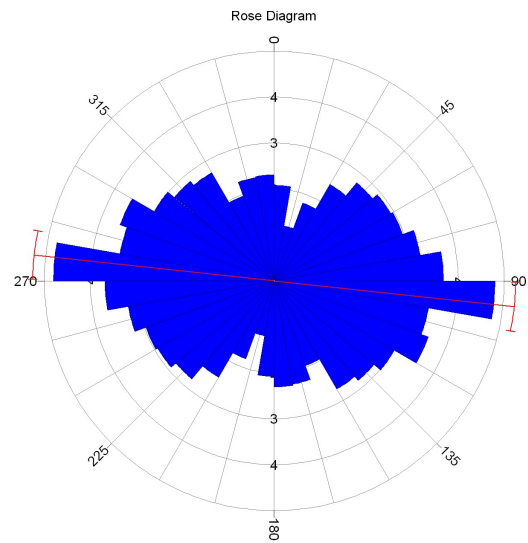


Figure 9. Directional rosette extracted from radar PALSAR DEM

Field data: To complete and validate the information provided by satellites, field campaigns were carried out. Various lithologies (granite, granodiorite, diorite) were identified and described during fieldwork (Fig). At landscape scale, they outcrop in circumscribed hills. At outcrop scale, they are

Lithology: A number of lithologies (granite, granodiorite, diorite) were identified and described during the various field campaigns (Fig.10). On a landscape scale, they outcrop in circumscribed hills. At outcrop level, they are arranged in slabs and blocks.



Figure 10. a) Granite dome outcrop; b) panoramic outcrop of study area; c and d: granodiorite block outcrop

The structures

Diaclases: Diaclases or dry joints are fractures that have affected different types of lithology, whether solid or non-magmatic. Diaclases are found throughout the study area. At the outcrop scale, diaclases are marked by the displacement or non-displacement of the various compartments. They have variable directions, but are generally oriented NE-SW and SE-NW in parts of the localities.

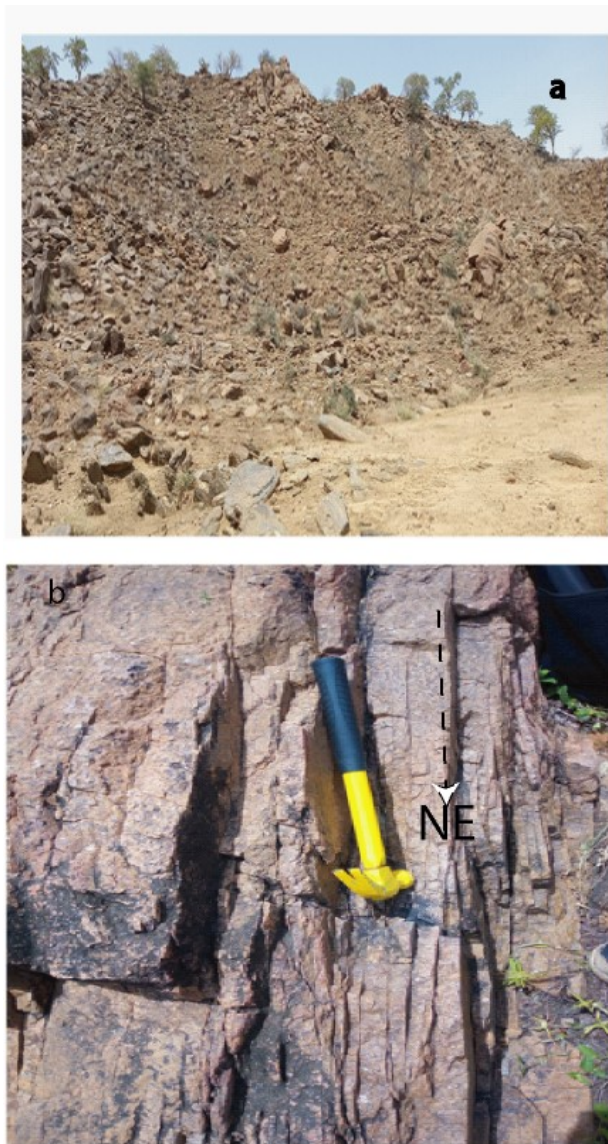


Figure 11. Photograph of the North Hadjer-Hadid sector. a) panorama of the sector; b) fracturing of the granites

All the measurements of the directions of the diaclases carried out in the field were used to establish the directional rosette (Fig. 12). Compilation of the fracturing data measured on the granites shows two main directions: between $N115^{\circ}$ and $N150^{\circ}$ E or SE-NW and $N25^{\circ}$ E to 45° E or NE-SW; and secondary directions (ENE-WSW, NNE-SSW and SSE-NNW), (Fig. 12).

DISCUSSION

Checking and validating the lithological map: The images generated from Landsat-8 and Aster DEM (DTM) were superimposed on the field data. This information was used to validate the lithological nature of the bedrock in our study area. Based on the colour composition and ratio bands, we were able to outline the lithological units with great precision and clarity. The granitoids (granites, granodiorites and diorites) are mapped in multicolour (red, yellow, brown, yellowish) in colour composition 651.

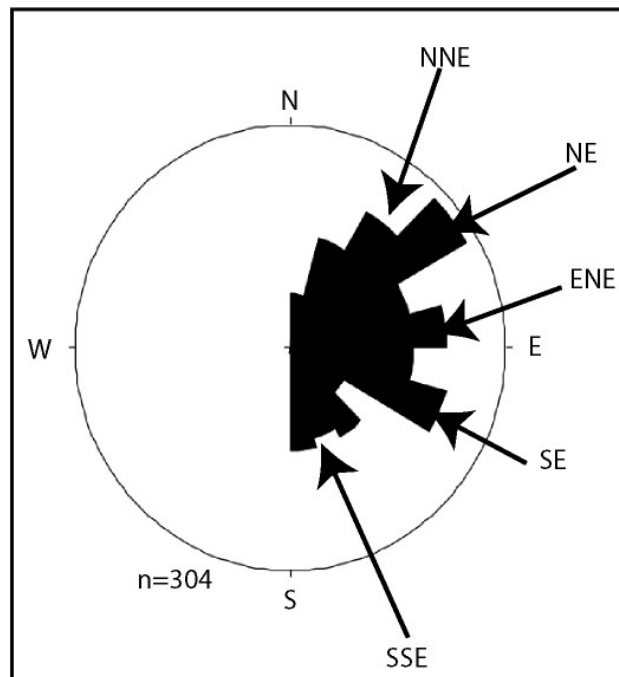


Figure 12. Fracture direction rosette for the entire study area

The sediments appear in greenish colour around the town of Adré, to the east of the map. Alluvial deposits appear in white. Vegetation is mapped in green.

Control and validation of lineament data: The aim of lineament control and validation is to compare the preferential directions of lineaments extracted from satellite images (Radar and Landsat-8), to compare them with those from existing tectonic and structural studies (Gsell J and Sonnet J., 1960) and with results from the field

Checking existing tectonic data for the study area: Lineament mapping using Radar and Landsat-8 images revealed two main fracturing directions: NE-SW and SE-NW. These directions are the same as those reported in the work of (Oussama, 2023); (Al-Djazouli et al., 2019). The geological map drawn up by (Gsell J and Sonnet J., 1960); (Schneider, 2001) shows a main vein direction: NE-SW. This direction corresponds to the main direction of the Precambrian basement of the Ouaddai massif.

Checking lineaments against field data: The aim of validating lineaments against field data is to physically identify lineaments that can be observed with the naked eye, lineaments that have already been mapped and lineaments of great importance in geology, such as shear corridors or faults. This method is the most suitable way of validating the lineaments. More than 300 fracture planes were measured in the field. Stereograms and directional rosettes show that the study area is organised into two fracture directions: $N115^{\circ}$ - 135° and $N45^{\circ}$ - 70° . These directions are identical to those generated by the Radar and Landsat-8 sensors. Image processing using remote sensing techniques is an important approach to geological and structural studies.

CONCLUSION

Geological and structural mapping using radar and Landsat data is a rapid and effective means of identifying and mapping geological structures in arid environments, especially when coupled with field data.

Conflicts of interest

The authors declare that there is no conflict of interest for this publication.

REFERENCES

- Al-Djazouli, M.O., Elmorabiti, K., Zoheir, B., Rahimi, A., Amellah, O., 2019. Use of Landsat-8 OLI data for delineating fracture systems in subsoil regions: implications for groundwater prospection in the Waddai area, eastern Chad. *Arab. J. Geosci.* 12, 1–15. <https://doi.org/10.1007/S12517-019-4354-8/METRICS>
- Baghdadi, Lasne, Nicolas, NGilles, Grandjean, Didier, Lahondère, PaillouYannick, P., 2005. apport de l'imagerie satellitaire radar pour l'exploration géologique en zones arides. *Sci. direct* 10.
- Bayouhd, M., Roux, E., Richard, G., Nock, R., 2015. Structural knowledge learning from maps for supervised land cover/use classification: Application to the monitoring of land cover/use maps in French Guiana. *Comput. Geosci.* 76, 31–40. <https://doi.org/10.1016/J.CAGEO.2014.08.013>
- Berraki, Bendaoud, F., Brahmi, B., Djemai, S; Kienast, J; Deroin, J., & Ouzegane, K., 2012. Cartographie et étude pétrographique et minéralogique des dykes de dolérites de l'in ouzzal (hoggar occidental, algérie). *Photo-Interpretation. Eur J Appl Remote Sens.*
- Chaussier, B.J., 1970. Carte minérale du Tchad. B.R.G.M.2^e ed. 82p
- Djerosse, F., Berger, J., Vanderhaeghe, O., Isseini, M., Ganne, J., Zeh, A., 2020. Neoproterozoic magmatic evolution of the southern Ouaddaï Massif (Chad). *Bull. la Société Géologique Fr.* 191, 34. <https://doi.org/10.1051/BSGF/2020032>
- Djerosse, Nenadji, F., 2018. Croissance et remobilisation crustales au Pan-Africain dans le sud du massif du Ouaddaï (Tchad). Thèse doct. Univ. Toulouse. 303p
- Djerosse, Nenadji, F., Rirabé, N., Ronang Baïsse, G., Ngarena Klamadji, M., Hisseine Malik, M., 2024. Lineament and Lithological Mapping of Meta-Sediments and Granitoids of Goz-Beïda (Eastern Chad) Based on Semi-Automatic Processing of Landsat 8 Oli/Tirs Images. *J. Geosci. Geomatics* 12, 80–86. <https://doi.org/10.12691/JGG-12-4-1>
- Doumnang, J-C., 2006. Géologie des formations néoprotérozoïques du Mayo Kebbi (Sud-Ouest du Tchad) : apport de la pétrologie et de la géochimie : implications sur la géodynamique au Panafricain. Thèse doct. Univ. Orléans. 223p
- El-Sawy, E.-S.K., Atef, Peter, Saoud, W., Atef, P ; Ibrahim, M., El-Bastawesyp, M.A., El-Saudp, W.A., 2016. Automated, manual lineaments extraction and geospatial analysis for Cairo-Suez district (Northeastern Cairo-Egypt), using remote sensing and GIS. *IJSET-International J. Innov. Sci. Eng. Technol.* 3.
- Fatma, B., Zahoua, H., 2022. Télédétection par imagerie Landsat-8 et Sentinel-2 dans la région des Eglabs; application de la cartographie géologique des feuilles au 1:200000 Gomez, C. 2004. Potentiels des données de télédétection multisources pour la cartographie géologique: Application à la région de Rehoboth (Namibie). Thèse doct. Laude Bernard - Lyon I. 210p
- Gsell J and Sonnet J., 1960, 1960. Carte géologique de reconnaissance au 1/500.000 et notice explicative sur la feuille Adre. Brazzaville. BRGM 42.
- Hammad, N., 2016. Cartographie géologique et analyse linéaire de la région d'El Kseïbat (Sahara du sud-ouest) à partir des images spatiales. Incidence sur l'exploration minière. *Estudios Geológicos. enero-junio 2016, 72(1), e049.* ISSN-L: 0367-0449. doi: <http://dx.doi.org/10.3989/egeol.42158.377>
- Hingue, N.V., Mbaigané, J.C.D., Diondoh, M., Mbaihoudou, D., 2024. Petrography and Geochemistry of the Farchana-Hadjerhadid Granitoids (Ouaddaï Massif, Eastern Chad). *Eur. J. Environ. Earth Sci.* 5, 8–15. <https://doi.org/10.24018/EJGEO.2024.5.4.473>
- Kruse, F.A., J.W.B., Huntington, J.F., 2003. Comparison of airborne hyperspectral data and EO-1 Hyperion for mineral mapping., *IEEE Trans. Geosci. Remote Sens.* 1388–1400.
- Kusnir, I., 1995. Géologie, ressources minérales et ressources en eau du Tchad ; Travaux.
- Miyouna, Timothée, Babezizonza, N.C., Florent, E.O., Medry, H., Nkodia, D.-V., Carmel, N., Tchiguina, B., Essouli, F.O., Kempena, A., Boudzoumou, F., 2020. Cartographie par traitement d'image satellitaire des linéaments du groupe de l'Inkisi en République du Congo : implications hydrogéologique et minière. *Afrique.* 17.
- Oussama, M.A.T., 2023. Etudes pétrographique et structurale des formations magmatiques et métamorphiques du massif du Ouaddaï (Axe Abéché – Adré). *Mém. Mast. Univ. N'Djamena.* 46p
- Pias, J., 1964. Carte pédologique de la reconnaissance au 1/200 000. feuille d'Abéché, Biltine et Oum-hadjer. N'Djamena. O.R.S.T.O.M. 209p.
- Schneider, J.L., 2001. Géologie, Archéologie, Hydrogéologie de la République du Tchad.. Carte de valorisation des eaux souterraines de la République du Tchad, 1/1500000, Direction de l'hydraulique, N'djamena. Vol. 2. 1100p
- Veyssière, G., 2019. Apport des mesures du radar à synthèse d'ouverture de Sentinel-1 pour. Toulouse.
- Yang'tshi, M., Olola, N., Lokilo, E.L., Ngungu, M., Yang'tshi, M.N., Nzambe, K.K., Ngungu, M.B., Matamba, R.J., Kunambu, C.M., Luemba, M.L., Kalonji, G.L., Ndaye Mudumbi, H., Ngbolua, K.-T.-N., 2018. Contribution de l'Imagerie Landsat 8 dans le repérage et la cartographie des linéaments aux environs de Madimba, dans l'Ouest Congolien (Kongo Central, République Démocratique du Congo). *Int. J. Innov. Sci. Res.* 38, 192–202.
